CHAPTER 7

CHAPTER 7

Deciphering Anti-Cancer Pathways: Molecular gene expression and bioinformatics analysis of protein-protein interaction of *S. virginianum* Leaf Extract and Melatonin in Breast Cancer Cells

7.1 Introduction

In this particular chapter, we analyzed molecular gene expression on experimental groups comprising MCF-7 and MDA-MB-231 cells. The aim was to elucidate the molecular pathways underlying the anti-proliferative effects of *Sv* leaf extract, both alone and in combination with melatonin.

Our study focused on the expression of *CASP3, CASP8,* and *CASP9* gene expression. *CASP8* is a component of the initiator caspases that initiates the extrinsic pathway of cell death (Ashkenazi, 2015; Bhat et al.,2023), while *CASP3* belongs to the execution caspases, mediates the intrinsic pathway (Loison et al., 2014, Bhat et al.,2023). Stimulation of intrinsic cell death leads to distinct and sequential effects on mitochondria, where *CASP9* can hinder cytochrome-C access to complex III, resulting in increased ROS production. Conversely, ROS production ceases when effector caspase activity is present (Cepero et al., 2005; Hajibabaie et al.,2023).

Melatonin is known for mitigating pathogenic inflammation by modulating various pathways, such as reducing TNF-α, IL-2, and IFN-γ release while elevating IL-4, IL-10, and IL-27 levels (Önde et al., 2022) Additionally, melatonin increases the expression of *BAX* and decreases *BCL2* expression in both MCF-7 and MDA-MB-231 cell lines (Önde et al., 2022). Moreover, it enhances the expression of autophagy markers Beclin-1, LC3, and p62 in these cell lines (Önde et al., 2022).

Furthermore, mRNA expression of matrix metalloproteinases (*MMP*s) is elevated in breast cancer cells compared to normal breast tissue. Among *MMP*s, *MMP*-2 and *MMP*-9 have garnered significant attention due to their role in cancer metastasis by degrading type IV collagen, a crucial component of the vascular basement membrane (Pyke et al., 1993). Studies have demonstrated a correlation between *MMP*2 and *MMP*9 expression levels, tumour staging and lymph node metastasis in breast cancer tissues (Mönig et al., 2001; Li et al., 2018). These *MMP*s are promising indicators for breast cancer prognosis and therapeutic strategies.

Table 7.1.1 lists the selected genes for the putative anti-cancer pathways, reinforcing the findings of *in vitro* anti-cancer activities observed in previous chapters.

Table 7.1.1: List of genes studied by Real time PCR

	Pathways	**Genes**	**References**
	Endogenous gene (Control)	ACTB (Beta-actin)	Suraweera et al.,2020
1.	Intrinsic apoptotic pathway	*BAX*: Pro-apoptotic marker *BCL2*: Anti-apoptotic marker	
2.	Extrinsic apoptotic pathway	*CASP3*: Effector caspase *CASP8*: Initiator caspase *CASP9*: Effector caspase	
3.	Matrix metalloproteinase	*MMP2, MMP9*	Li et al.,2017
4.	Anti-inflammatory activity	*IL4,IL10*	Fasoulakis et al.,2018

Along with molecular gene expression studies, *in silico* the biochemical pathway analysis was also performed to get better understanding of protein-protein interactions (PPI) in breast cancer. Biochemical analysis is vital for comprehending the complex molecular mechanisms that regulate biological processes (Elbashir et al.,2023). Researchers can gain valuable

insights into cellular systems by deconstructing pathways and clarifying protein-protein interactions (PPI). Exploring PPI networks uncovers the complex structure and dynamic characteristics of cellular systems, providing insight into essential protein centers and their interrelated roles (Elbashir et al.,2023). Advancements in high-throughput technologies have resulted in vast amounts of PPI data, necessitating sophisticated computational approaches for examination and understanding protein-protein interaction. Cytoscape is a powerful bioinformatics tool that is widely utilized for the visualization and analysis of molecular interaction networks (Oumeddour ,2023).

In this chapter, we investigated the selected candidate gene expression profile of MCF-7 and MDA-MB-231 cell lines exposed to Sv leaf extract alone and combined with melatonin. This analysis aimed to elucidate the intricate molecular mechanisms modulated by the experimental treatments. The present study also highlights a methodical approach to biochemical analysis, particularly emphasizing pathway analysis and PPI exploration using Cytoscape and CytoHubba tools integration.

7.2 Materials and methods

TRI Reagent (Himedia MB566), Chloroform (SRL 96712), Isopropanol (SRL 67800), ethanol, DEPC water (Himedia TCL016), Verso cDNA Synthesis kit Thermo Scientific Cat-AB14534A, Primer Eurofins Genomics U.S., PowerUp™ SYBR™ Green Master Mix for qPCR Applied Biosystems (Cat#A25742).

Below are the details of the experimental groups for this chapter:

Experimental group	**MCF-7**		**MDA-MB-231**	
1	Control	0.2% DMSO	Control	0.2% DMSO
2	*Sv* leaf aqueous extract : E Sub IC_{50}	5 µg/mL	*Sv* leaf methanolic extract : E Sub IC_{50}	6 µg/mL
3	*Sv* leaf aqueous extract : E IC_{50}	10 µg/mL	*Sv* leaf methanolic extract : E IC_{50}	12 µg/mL
4	Melatonin : Sub IC_{50}	12 µg/mL	Melatonin : Sub IC_{50}	24 µg/mL
5	Melatonin : IC_{50}	24 µg/mL	Melatonin : IC_{50}	48 µg/mL
6	(E +Mel): Sub IC_{50}	(5+12) µg/mL	(E +Mel) : Sub IC_{50}	(6+12) µg/mL
7	(E + Mel): IC_{50}	(10+24) µg/mL	(E + Mel) : IC_{50}	(12+24) µg/mL
8	Doxorubicin(Positive control)	24 µg/mL	Doxorubicin(Positive Control)	50 µg/mL

Gene expression study: Real-time PCR analysis (Wagner et al.,2013)

Real-time PCR involves continuous monitoring of amplification product accumulation as the reaction progresses, with product measurement after each cycle. Specific primers tailored to the experiment and PCR reagents initiate the amplification reactions. In the current study, the PCR products were analysed utilising SYBR® Green. This dye binds to the minor groove of double-stranded DNA. The fluorescence intensity increases when SYBR Green attaches to double-stranded DNA, with fluorescence rising as more double-stranded amplicons are generated.

7.2.1 RNA Extraction

RNA extraction was performed using the traditional phenol chloroform separation method as described by Chomczynski et al. (1987). The extraction process comprised several stages including lysis, phase separation, precipitation, washing, and elution.

7.2.1.2 Experimental design

1.5 x 10^5 cells/well of MCF-7 and MDA-MB-231 cells were seeded in a 6-well plate. Upon reaching confluency, cells were treated for 24 hr. RNA was isolated from both untreated and treated cells of MCF-7 and MDA-MB-231 cell lines. Before RNA extraction, surface sterilisation was performed to minimise the RNase activity of environmental components. Cells were trypsinized and collected in a 1.5 mL microcentrifuge tube for RNA extraction. Subsequently, 1 mL of TRI reagent was added to each tube and vortexed for 2 min. Then, 150 µL of chloroform was added to each tube, followed by a 5 min incubation at room temperature. After vigorous shaking and vortexing for 1 min, the tubes were subjected to cooling centrifugation at 12,000 rpm for 15 min at 4°C. Following centrifugation, three distinct layers were observed, with the top clear layer containing RNA. This layer was collected in a new tube, and an equal amount of isopropanol was added for precipitation. After incubating at -20°C for 20 min, the tubes were centrifuged at 7,500 rpm for 5 min to

pellet the RNA. The resulting RNA pellet was washed several times with absolute ethanol (two to three times) to remove any remaining alcohol-soluble contaminants. Centrifugation was performed at 5,000 rpm for 5 min during each washing step. After washing, the alcohol was decanted, and the tubes were air-dried to remove excess alcohol. The RNA pellet was then resuspended in DEPC water and stored at -20°C for cDNA synthesis.

Quantifying and determining the 260/280 ratio of the RNA samples was performed using a NanoDrop spectrophotometer (NanoDrop Technologies, USA). All RNA samples were adjusted to 1 μg/mL concentration using DEPC water.

7.2.2 cDNA Synthesis by RT-PCR (Reverse Transcription-Polymerase chain reaction)

In this assay, RNA undergoes conversion to its complementary DNA sequence through the action of reverse transcriptase enzyme, followed by amplification of the resulting cDNA using the Verso cDNA synthesis kit (Thermo Scientific: cat#AB14534A).

7.2.2.1 Experimental Design

Reagents were dispensed into PCR tubes according to the respective experimental groups. Stock solution contents were thawed and combined as per the instructions provided by the kit manufacturer (see Table 7.2.1). Amplification was conducted in a thermocycler (Invitrogen, USA) for a specified number of cycles using the program set up for cDNA synthesis outlined in Table 7.3. The volume of each component was adjusted for a final reaction volume of 20 μL.

Table 7.2.1: cDNA synthesis cocktail preparation		
Components	**Final concentration**	**Volume (µL)**
5X RT Buffer	1X	4.0
20mM dNTP mixture	500 µM each	1.6
Random Primers (400 ng/µL)	-	4.0
RT Enzyme mix with RNase Inhibitor	-	2.0
Nuclease free water (NFW)	-	8.4
Template (RNA)	1µg	1.0
Total system volume		**20**

Table 7.2.2: Program setup for cDNA Synthesis		
Stages	**Temperature °C**	**Time (Sec)**
Denaturation	95	10:00
Annealing	42	30:00
Primer extension	85	05:00
Final product	4	∞

7.2.3 Quantitative Real-Time PCR: Amplification of Target gene and endogenous gene

For quantitative Real-Time PCR, SYBR green chemistry was utilized. Following each PCR cycle, the amplicons were quantified by measuring the fluorescence generated, expressed as the Ct value. The relative fold change in gene expression for each target gene was calculated using the $2^{-\Delta\Delta Ct}$ method, wherein the Ct value of an endogenous gene served as the reference (Schmittgen et al., 2008).

7.2.3.1 Experimental Design

The prepared cDNA, generated as described previously, served as the template for the Real-Time PCR assay. The primers and conditions were designed using NCBI (https://www.ncbi.nlm.nih.gov/tools/primer-blast/) and the validation was done using OligoCalc online available software (http://biotools.nubic.northwestern.edu/OligoCalc.html). The primer sequences for all the target gene and the endogenous gene are provided in Table 7.2.3. A master mix was prepared using SYBR Green master mix (Applied Biosystems, cat# A25742) along with forward and reverse primers in PCR tubes, following the manufacturer's instructions (Table 7.2.3 and Table 7.2.4).

Subsequently, 1 µL of cDNA was added directly to each well in the PCR plate. The PCR plate temperature was maintained using a 96-well frosty box. The reaction was conducted in a 10 µL system using a Real-Time PCR system (QuantStudio 12K Flex / Fast 96-Well Block (0.1mL). The program setup for amplification is outlined in Table 7.2.5.

Table 7.2.3: Primer details for target and endogenous gene

Gene	Forward primer	Reverse primer
ACTB	CACCATTGGCAATGAGCGGTTC	AGGTCTTTGCGGATGTCCACGT
BAX	CCCGAGAGGTCTTTTTCCGAG	CCAGCCCATGATGGTTCTGAT
BCL2	CTGCACCTGACGCCCTTCACC	CACATGACCCCACCGAACTCAAAGA
CASP3	TTAATAAAGGTATCCATGGAGAACACT	TTAGTGATAAAAATAGAGTTCTTTTGTGAG
CASP8	GGTCACTTGAACCTTGGGAA	AGGCCAGATCTTCACTGTCC
CASP9	GTGGACATTGGTTCTGGAGGAT	CGCAACTTCTCACAGTCGATG
MMP2	CTGCATCCAGACTTCCTCAG	GGTCCTGGCAATCCCTTTGT
MMP9	CCTGGGCAGATTCCAAACCT	CAAAGGCGTCGTCAATCACC
IL10	CACATCAGGGGCTTGCTCTT	TGAGCTGTGCATGCCTTCTT
IL4	TGAACAGCCTCACAGAGCAG	TGTGTTCTTGGAGGCAGCAA

Table 7.2.4: Cocktail preparation for Real time-PCR analysis	
Component	**Volume (µL)**
SYBR master mix	5.0
Forward primer	0.5
Reverse Primer	0.5
Nuclease free Water	3.0
cDNA (in each well)	1.0
Total system Volume	10.0

Table 7.2.5: Program setup for Real-Time PCR amplification			
Stages	**Temperature °C**	**Time (Sec)**	**Cycle**
UDG Activation	50	02:00	1 cycle
DNA Polymerisation	95	02:00	
Denaturation	95	15:00	39 cycle
Annealing	56	15:00	
Extension	72	1:00	
Final	4	∞	40 cycles

7.2.4 Protein-protein interaction network analysis

The STRING (v11.5) (https://string-db.org/) biological online database was utilized for the known and predicted protein-protein interactions. The STRING database is a valuable resource that consolidates information from multiple sources, enabling scientists to make accurate predictions about the functional interactions of proteins (Szklarczyk et al.,2023).

7.2.5 Selection of HUB genes

Cytohubba explores the significance of the protein HUB (Su et al.,2023). It provides a range of topological algorithms for ranking nodes using different centrality measures, such as degree, betweenness, and closeness centrality (Su et al.,2023). Through the identification of highly connected nodes or "hub proteins" within PPI networks, CytoHubba assists in prioritizing candidate proteins for additional experimental validation and functional characterization. The extraction of hub genes was performed using the CytoHubba software, a plug-in for CYTOSCAPE V3.10.1 then the most crucial hub genes were identified (Oumeddour ,2023).

7.2.6 Statistical analysis

The statistical analysis of the obtained data was conducted using GraphPad Prism 8.0 software. The data are presented as fold change compared to untreated cells, with values represented as mean ± SEM from three individual experiments. Each value of untreated cells and treatment groups were subjected to one-way ANOVA. Significance levels were determined by comparing the data to untreated cells, where * represents $p < 0.05$, ** represents $p < 0.01$, and *** represents $p < 0.005$, and **** represents $p < 0.001$.

7.3 Result

Gene expression alteration was validated through Real-Time PCR analysis of nine selected genes (Table 7.1.1) for both MCF-7 and MDA-MB-231 cells. These cells were treated with varying concentrations of leaf aqueous extract of *Sv* (IC_{50} and Sub IC_{50}) and/or melatonin (IC_{50} and Sub IC_{50}). For MCF-7 cells, the treatments included leaf aqueous extract of *Sv*, while for MDA-MB-231 cells, leaf methanolic extract of *Sv* was used. In each case, both IC_{50} and Sub IC_{50} concentrations of *Sv* extract and melatonin were employed for treatment.

7.3.1 Gene expression study for ER+/PR+ breast cancer cell line: MCF-7

The relative expression of *BAX* was significantly upregulated in each group as compared to control (untreated cells). In case of combinational groups, sub IC_{50} concentration of E+Mel group showed higher *BAX* expression as compared to individual extract and melatonin treated groups (Figure 7.3.1). In case of *BCL2* and *MMP2* and *MMP9*, the mRNA expression showed significantly lower expression in all groups compared to control (Figure 7.3.1, Figure 7.3.3).

The mRNA expression of *CASP3* and *CASP9* were upregulated in all treated groups compared to control. Additionally, *CASP9* and *CASP3* were shown comparatively higher in case of combinational groups as compared to individually treated group. *CASP8* mRNA expression was upregulated in all treated groups compared to control except in melatonin (IC_{50} and sub IC_{50}) treated cells. Additionally, for Caspases, it was noteworthy that the combinational treatment resulted in higher expression compared to individual treatment of *Sv* leaf extract and melatonin in the cells (Figure 7.3.2).

The mRNA *IL10* expression was comparatively higher in all groups except the extract (IC_{50}) individual and E + Mel combinational group (Figure 7.3.4). The significant elevated expression was observed in E + Mel sub IC_{50} combination group ($p<0.05$) and doxorubicin treated group ($p<0.05$) as compared to that of control. The mRNA expression of *IL4* showed elevated levels in case of all the groups compared to control. There was no significant difference among *IL4* mRNA expression among individual treatment and combinational treated groups (IC_{50}).

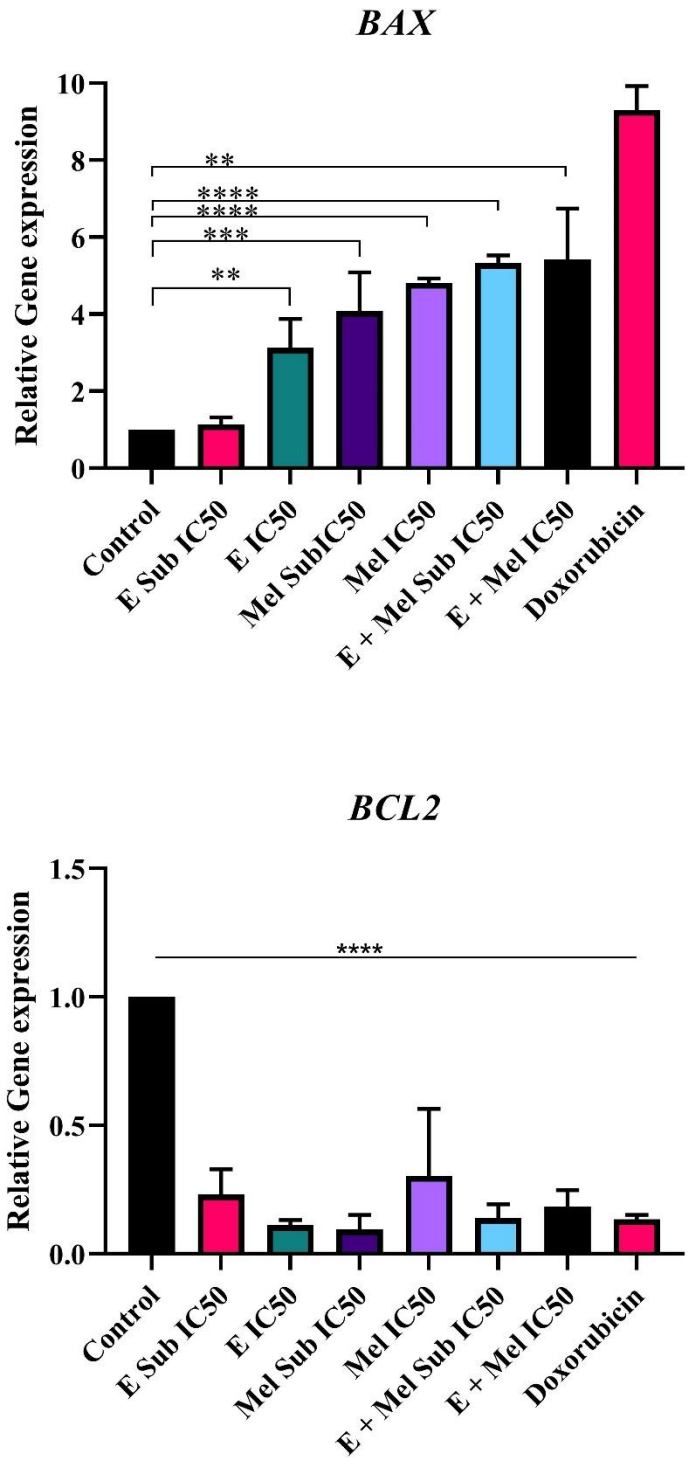

Figure 7.3.1: Gene expression study of *BAX and BCL2* of MCF-7 experimental groups using real time PCR

Significance levels were determined by comparing the data to untreated cells, mean ± SEM(n=3). where ** represents $p < 0.01$, and *** represents $p < 0.005$, and **** represents $p < 0.001$.

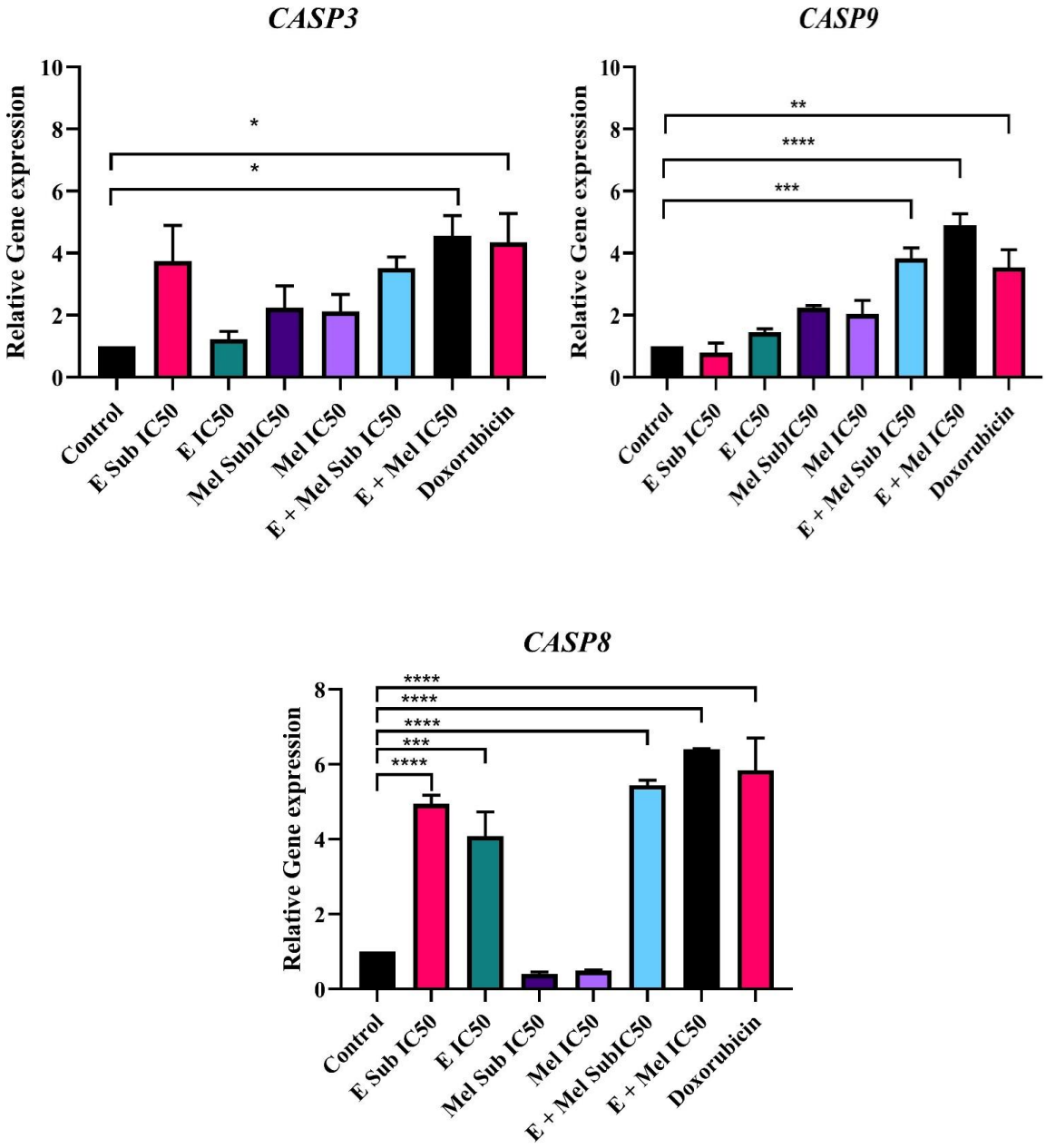

Figure 7.3.2: Gene expression study of *CASP3, CASP8* and *CASP9* of MCF-7 experimental groups using real time PCR

Significance levels were determined by comparing the data to untreated cells, mean ± SEM(n=3). where ** represents $p < 0.01$, and *** represents $p < 0.005$, and **** represents $p < 0.001$.

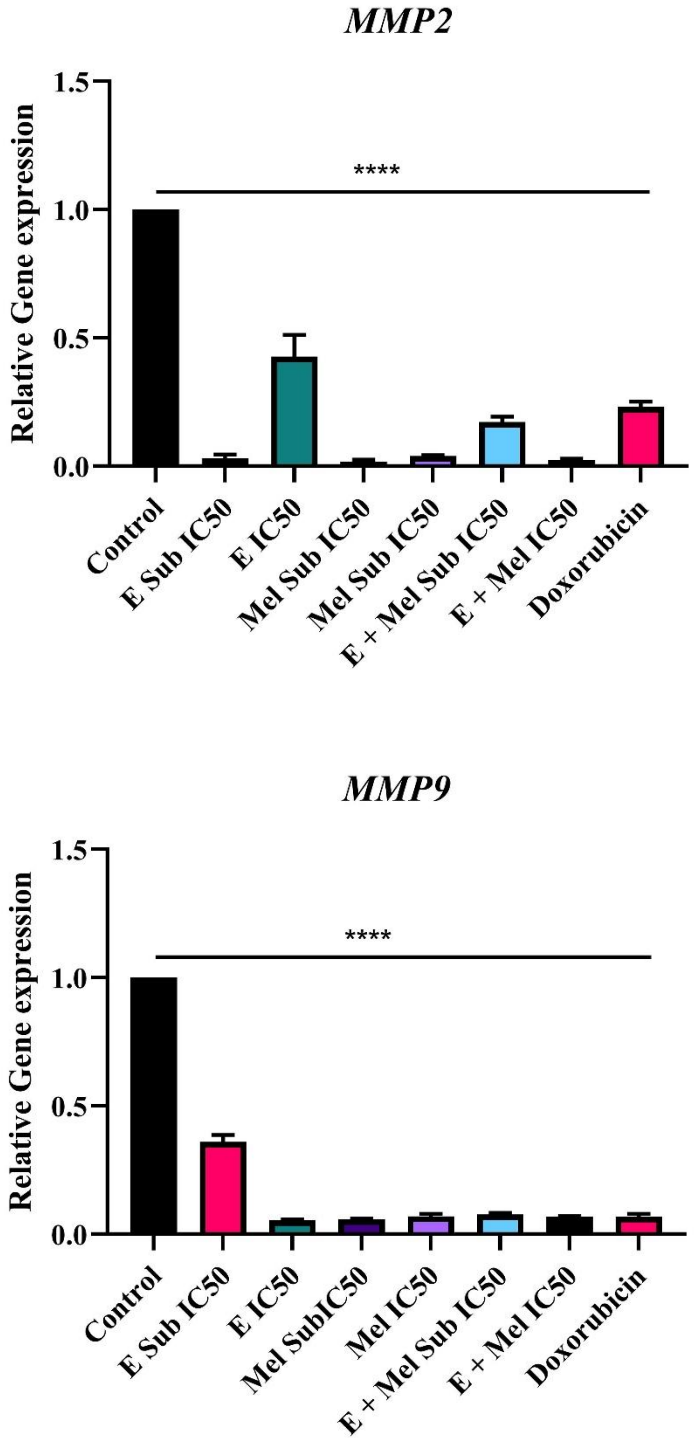

Figure 7.3.3: Gene expression study of *MMP2* and *MMP9* of MCF-7 experimental groups using real time PCR

Significance levels were determined by comparing the data to untreated cells, mean ± SEM (n=3 **** represents $p < 0.001$.

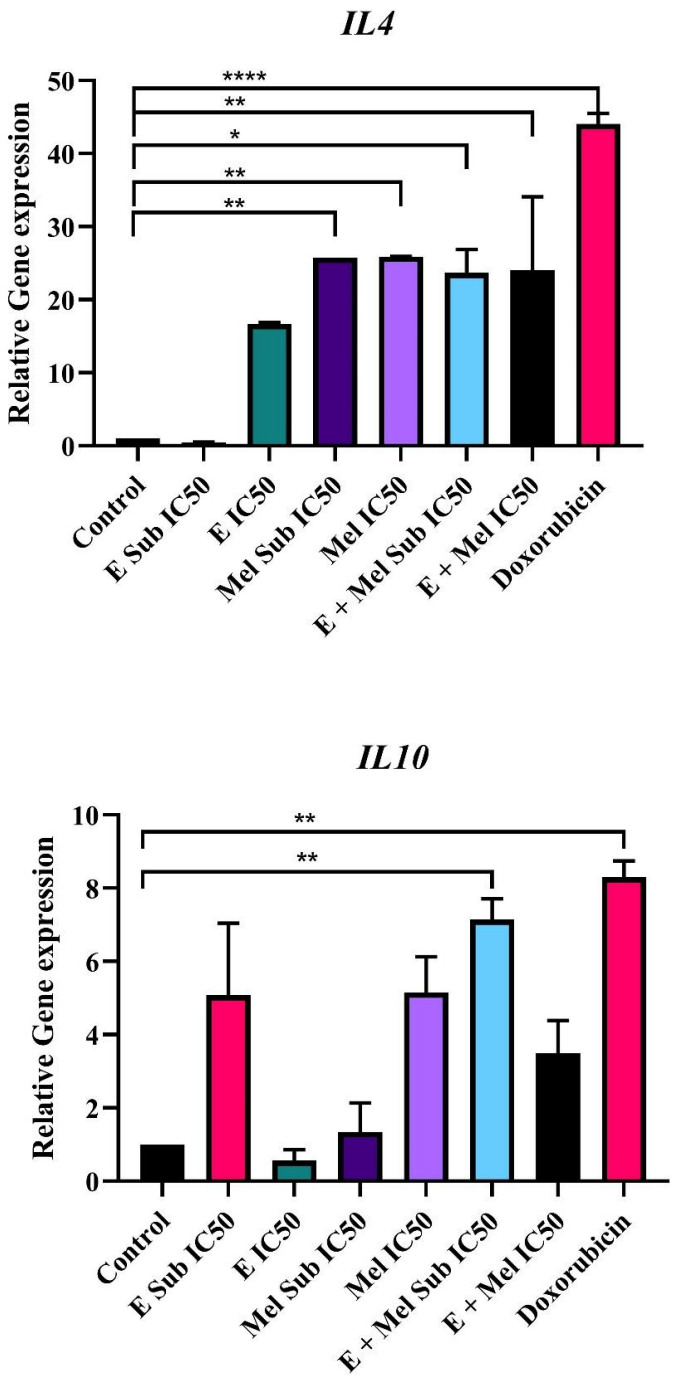

Figure 7.3.4: Gene expression study of *IL4* and *IL10* of MCF-7 experimental groups using real time PCR

Significance levels were determined by comparing the data to untreated cells, mean ± SEM(n=3). where * represents p <0.05, ** represents p < 0.01, and *** represents p < 0.005, and **** represents p < 0.001.

Table 7.1.1: Gene expression study for MCF-7 : Data represent fold change values.

	BAX	***BCL2***	***CASP3***	***CASP8***	***CASP9***	***MMP2***	***MMP9***	***IL4***	***IL10***
Control	1.00 ±0.00	1.00 ±0.00	1.00 ±0.00	1.00 ±0.00	1.00 ±0.00	1.00 ±00	1.00 ±0.00	1.00 ±0.00	1.00±0.00
E Sub IC_{50}	**1.14 ±0.18^{a}**	**0.23 ±0.1**	3.75±1.98	**4.94 ±0.41^{a}**	1.45 ±0.54	**0.03 ±0.01^{d}**	**0.36 ±0.05^{d}**	0.45 ±0.17	5.08 ±3.4
E IC_{50}	**3.13 ±0.75^{b}**	**0.11 ±0.02**	1.23 ±0.43	**4.08 ±1.12^{b}**	2.23 ±0.19	**0.43 ±0.15^{d}**	**0.05 ±0.01^{d}**	16.67 ±0.39	0.56 ±0.52
Mel SubIC_{50}	**4.08 ±1.01^{d}**	**0.09 ±0.06**	2.24 ±0.13	0.40 ±0.09	2.24 ±0.13	**0.02 ±0.01^{d}**	**0.06 ±0.0^{d}**	**25.78 ±0^{b}**	1.35 ±0.36
Mel IC_{50}	**4.82 ±0.11^{d}**	**0.30 ±0.26**	2.12 ±0.96	0.49 ±0.03	2.03 ±0.77	**0.04 ±0.01^{d}**	**0.07 ±0.02^{d}**	**25.90 ±0.08^{b}**	4.16 ±2.3
E + Mel Sub IC_{50}	**5.33 ±0.20^{d}**	**0.14 ±0.05**	**3.52 ±0.63^{c}**	**5.44 ±0.24^{d}**	**3.84 ±0.58^{c}**	**0.17 ±0.04^{d}**	**0.08 ±0.01^{d}**	**23.68 ±5.6^{a}**	**7.14 ±0.99^{b}**
E + Mel IC_{50}	**2.75 ±0.98**	**0.18 ±0.06**	**4.56 ±1.13^{a}**	**6.40 ±0.04^{d}**	**4.90 ±0.64^{d}**	**0.02 ±0.01^{d}**	**0.07 ±0.0^{d}**	**24.05 ±7.4^{a}**	0.16 ±0.07
Doxorubicin	1.30 ±0.08	0.13 ±0.02	4.35 ±1.62	5.84 ±1.49	3.54 ±0.98	0.23 ±0.04	0.07 ±0.02	44.05 ±2.51	8.29 ±0.78

Significance levels were determined by comparing the data to untreated cells, mean ± SEM(n=3). where '**a**' represents $p < 0.05$, '**b**' represents $p < 0.01$,'**c**' represents $p < 0.005$, and **'d'** represents $p < 0.001$.

7.3.2 Gene expression study for Triple negative breast cancer cell line: MDA-MB-231

In the triple-negative breast cancer cells, MDA-MB-231, the expression of *BAX* was upregulated in all treated groups compared to the control group. The highest expression of *BAX* was observed in the combinational IC_{50} group, which was also significant (***$p < 0.001$). *BCL2* expression was reduced in all treatment groups, although not significantly (Figure 7.3.5).

Regarding the mRNA expression of caspases, the combinational IC_{50} group showed the highest expression for *CASP3* ($p<0.05$), *CASP8* ($p < 0.05$), and *CASP9* ($p < 0.005$) (Figure 7.3.6). The fold change graphs for MMPs demonstrated that MMP expression was reduced in all treatment groups compared to the untreated group (Figure 7.3.7). The *IL4* fold change graphs showed that *IL4* expression increased in the extract and Melatonin IC_{50} treated groups and Combinational Sub IC_{50} treated groups, while for *IL10*, the fold change increased in all treatment groups except the Combinational IC_{50} group (Figure 7.3.8).

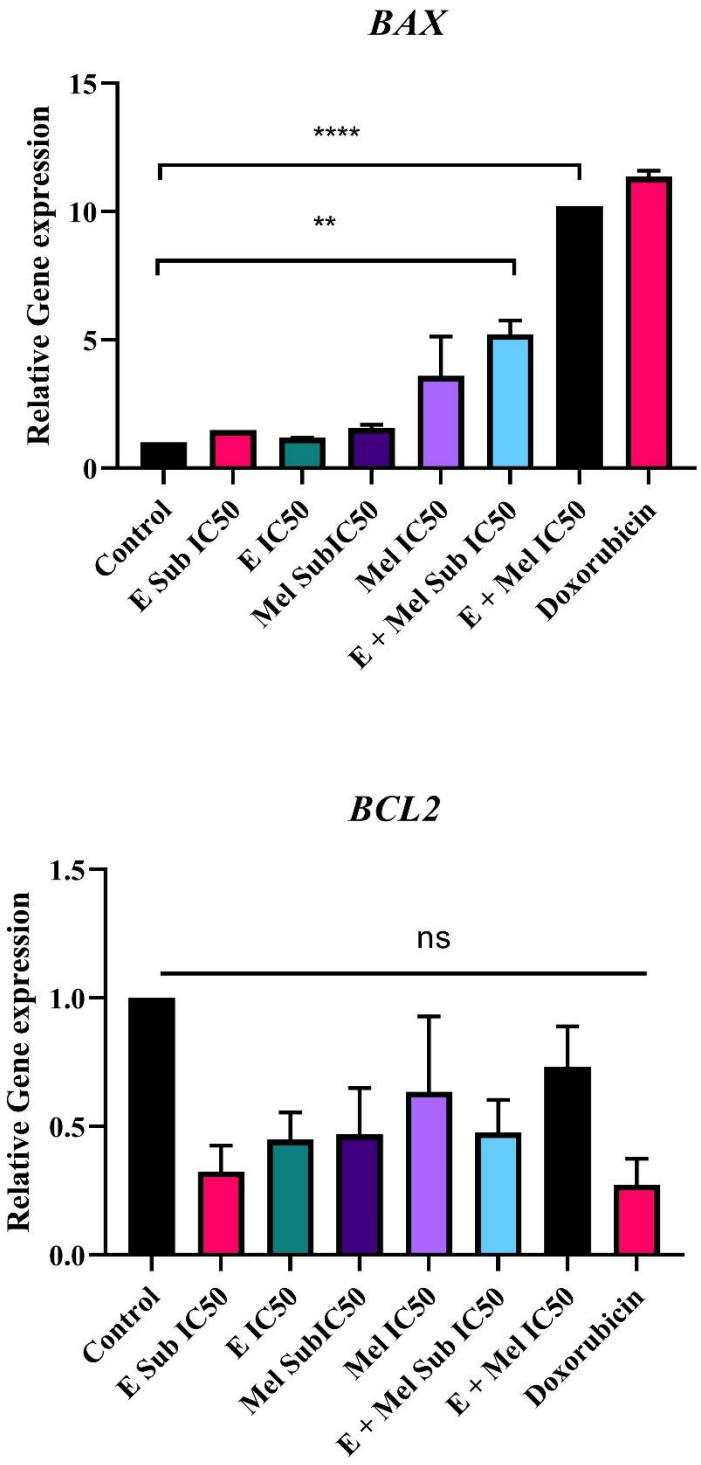

Figure 7.3.5: Gene expression study of *BAX* and *BCL2* of MDA-MB-231 experimental groups using real time PCR

Significance levels were determined by comparing the data to untreated cells, mean ± SEM(n=3). where ** represents $p < 0.01$, **** represents $p < 0.001$ and 'ns' represents non-significant.

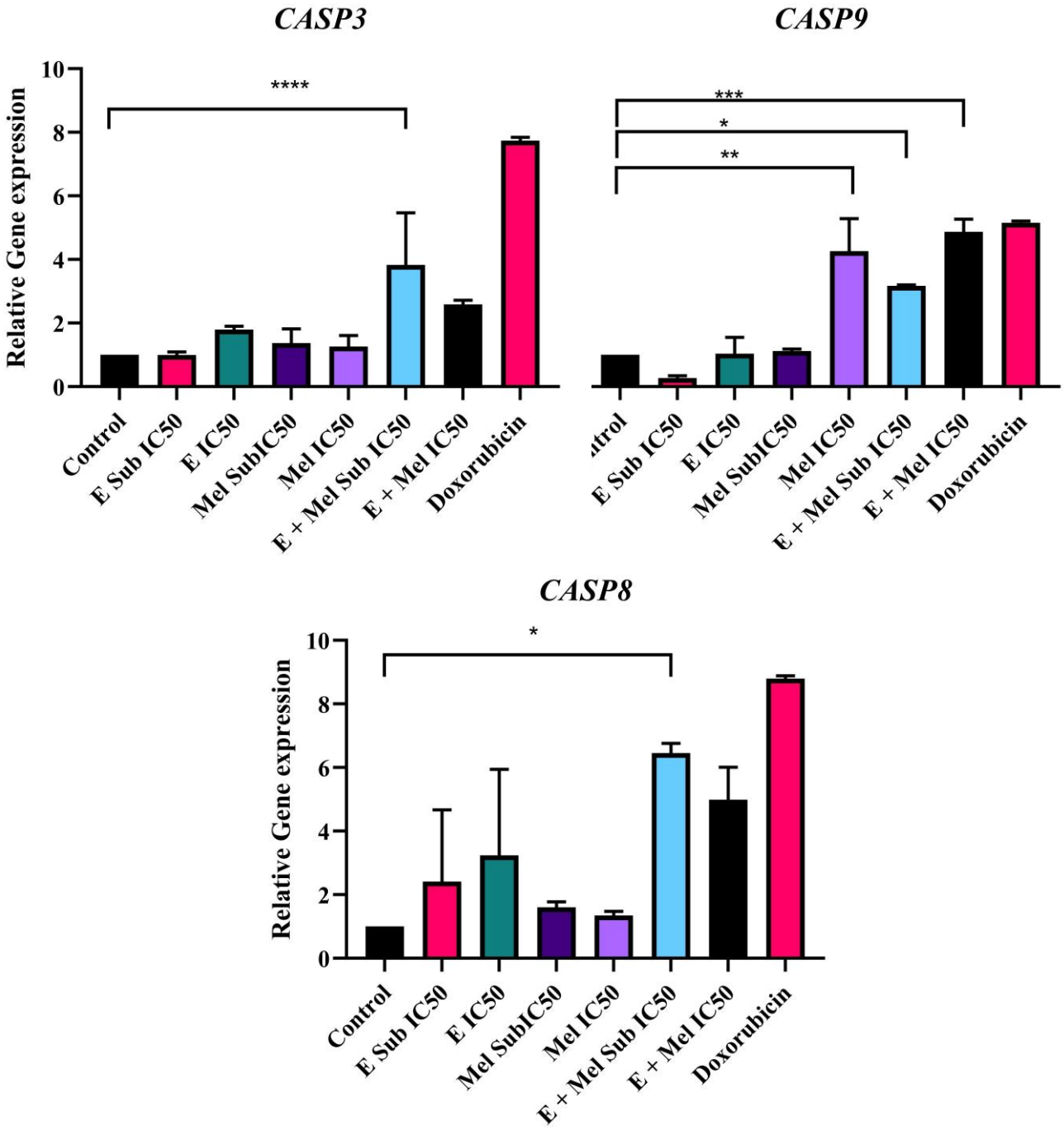

Figure 7.3.6: Gene expression study of *CASP3, CASP8* and *CASP9* of MDA-MB-231 experimental groups using real time PCR

Significance levels were determined by comparing the data to untreated cells, mean ± SEM(n=3). where * represents p <0.05,** represents p < 0.01, and *** represents p < 0.005, and **** represents p < 0.001.

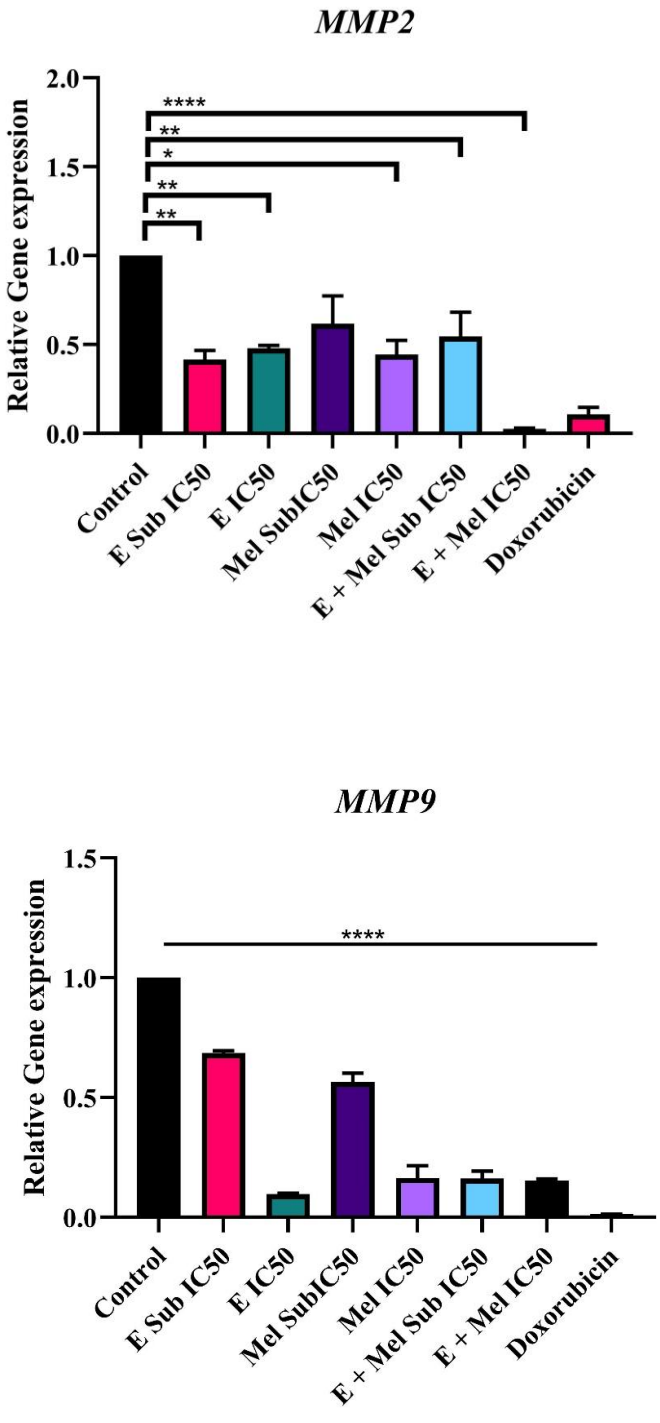

Figure 7.3.7: Gene expression study of *MMP2* and *MMP9* of MDA-MB-231 experimental groups using real time PCR

Significance levels were determined by comparing the data to untreated cells, mean ± SEM(n=3). where **** represents $p < 0.001$ and 'ns' is non-significant.

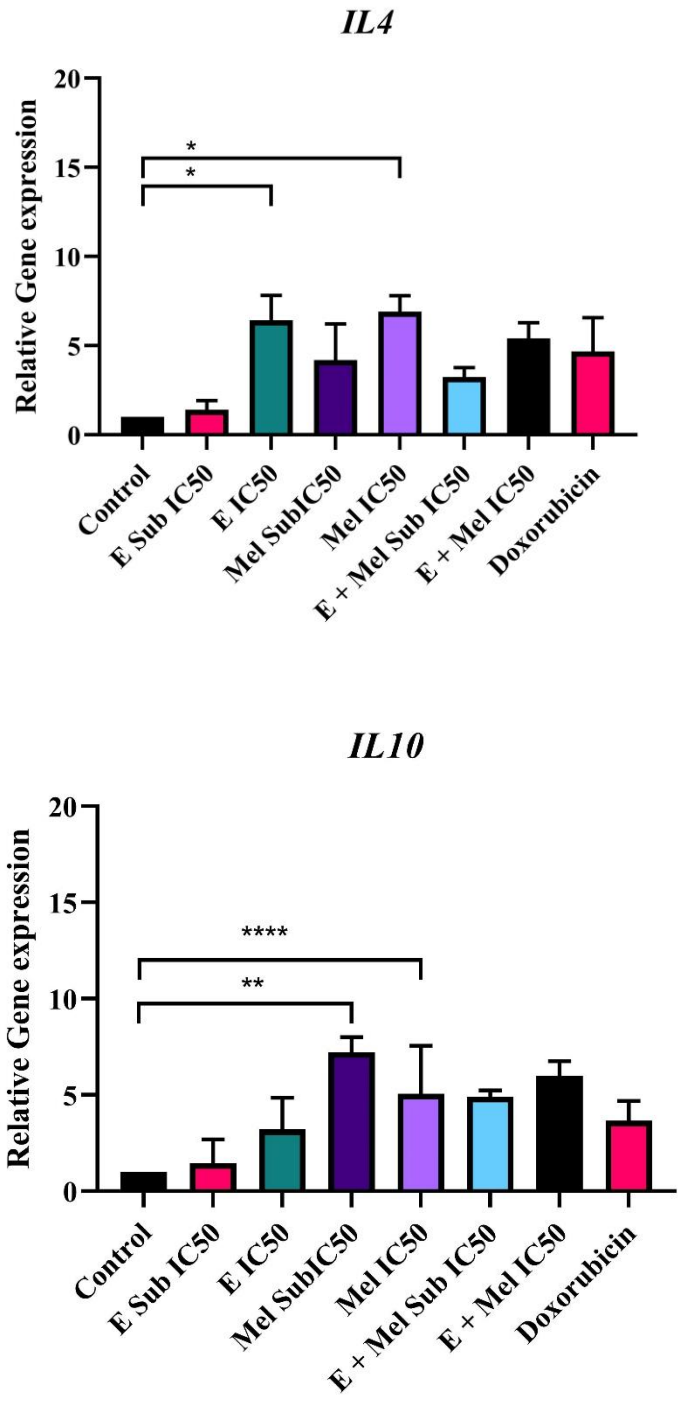

Figure 7.3.8: Gene expression study of *IL4* and *IL10* of MDA-MB-231 experimental groups using real time PCR

Significance levels were determined by comparing the data to untreated cells, mean ± SEM(n=3). where ** represents $p < 0.01$, and *** represents $p < 0.005$, and **** represents $p < 0.001$.

Table 7.3.2: Gene expression study for MDA-MB-231 : Data represent fold change values									
	BAX	*BCL2*	*CASP3*	*CASP8*	*CASP9*	*MMP2*	*MMP9*	*IL4*	*IL10*
Control	1.00 ±00	1.00 ±0.00	1.00 ±0.00	1.00±0.00	1.00 ±0.00	1.00 ±00	1.00 ±0.00	1.00 ±0.00	1.00±0.00
E Sub IC_{50}	1.48 ±0.00	0.32 ±0.18	1.00 ±0.17	2.41±0.96	0.27 ±0.13	**0.42 ±0.09^{b}**	0.69 ±0.02	1.41 ±0.89	1.45 ±0.63
E IC_{50}	1.19 ±0.01	0.45 ±0.18	0.79 ±0.19	3.24±1.23	1.04 ±0.12	**0.48 ±0.03^{b}**	0.10 ±0.01	**6.42 ±1.9^{d}**	3.21 ±0.84
Mel SubIC_{50}	1.56 ±0.80	0.47 ±0.31	0.70 ±0.25	1.60±0.30	1.12 ±0.01	**0.68 ±0.33^{a}**	0.57 ±0.06	4.20 ±2.86	**7.23 ±1.34^{b}**
Mel IC_{50}	3.59 ±2.86	0.63 ±0.15	0.93 ±0.15	1.34±0.4	**4.26 ±1.78^{b}**	0.98 ±0.46	0.16 ±0.09	**6.9 ±1.28^{d}**	**11.72 ±2.05^{d}**
E + Mel Sub IC_{50}	**5.22 ±0.92^{b}**	0.48 ±0.22	**3.83 ±2.84^{d}**	**6.45±0.63^{a}**	**3.17 ±0.06^{a}**	**0.55 ±0.24^{b}**	0.16 ±0.05	3.23 ±0.75	4.90 ±0.58
E + Mel IC_{50}	**10.22 ±0.00^{d}**	0.73 ±0.22	1.26 ±0.97	4.98±5.2	**4.87 ±0.68^{c}**	**0.03 ±0.01^{d}**	0.15 ±0.01	5.4 ±1.23	0.31 ±0.25
Doxorubicin	11.02 ±0.28	0.27 ±0.11	7.74 ±0.19	8.97±1.47	1.15 ±0.11	0.37 ±0.45	0.01 ±0.0	4.67 ±2..6	3.66 ±1.78

Significance levels were determined by comparing the data to untreated cells, mean ± SEM(n=3). where '**a**' represents $p < 0.05$, '**b**' represents $p < 0.01$,'**c**' represents $p < 0.005$, and **'d'** represents $p < 0.001$.

7.3.3 Analysis PPI Network construction

The STRING database was used to analyze selected target genes. The genes are subjected for the protein-protein interaction network construction. It was observed 57 nodes (genes) and 778 edges (interaction) (Table 7.3.3, Figure 7.3.9). Key targets were identified by Cytoscape 10.1 software. Hub proteins are identified using cytohubba software. The first 10 hub genes were selected by degree method. They are namely TNF, IL1B, BCL2, IL6, IL18, IL1A, CASP8, TLR4, TLR2, *IL10* (Figure 7.3.10). The red color code indicates the anti-apoptotic proteins (TNF,BCL2) and pro-inflammatory (IL1B), while yellow and orange coloured box indicates pro apoptotic proteins (TLR2,TL4,CASP8,IL6,IL10,IL18,TLR4,TLR6) (Figure 7.3.10).

The selected HUB genes were ranked on the basis of score which indicates the interaction proximity in pathway analysis (Table 7.3.4). Out of 10 HUB genes, TNF showed highest score which is 47 while IL10 shows lowest score which is 39.

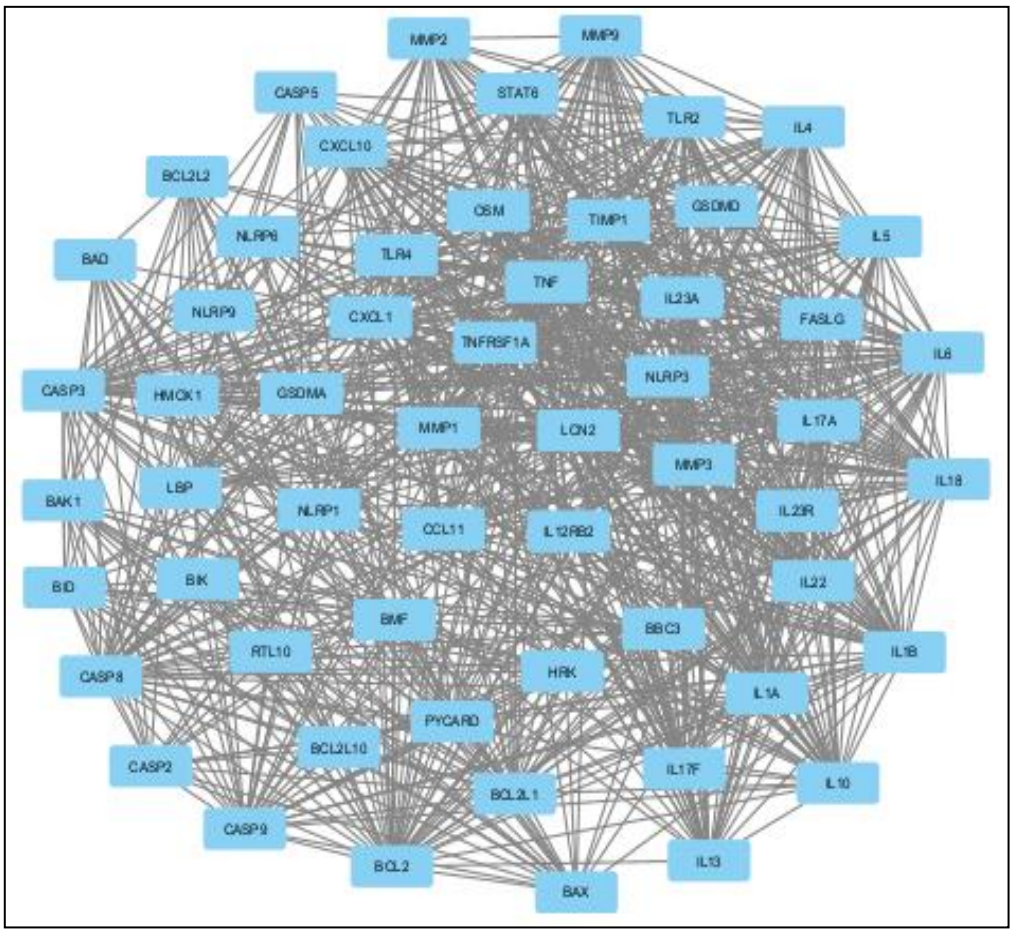

Figure 7.3.9: PPI network analysis using Cytoscape 10.1 software

Table 7.3.3 Network status	
Number of nodes:	57
Number of edges:	778
Average node degree	27.3
Avg. local clustering coefficient	0.802
Expected number of edges:	156
PPI enrichment p-value	< 1.0e-16.

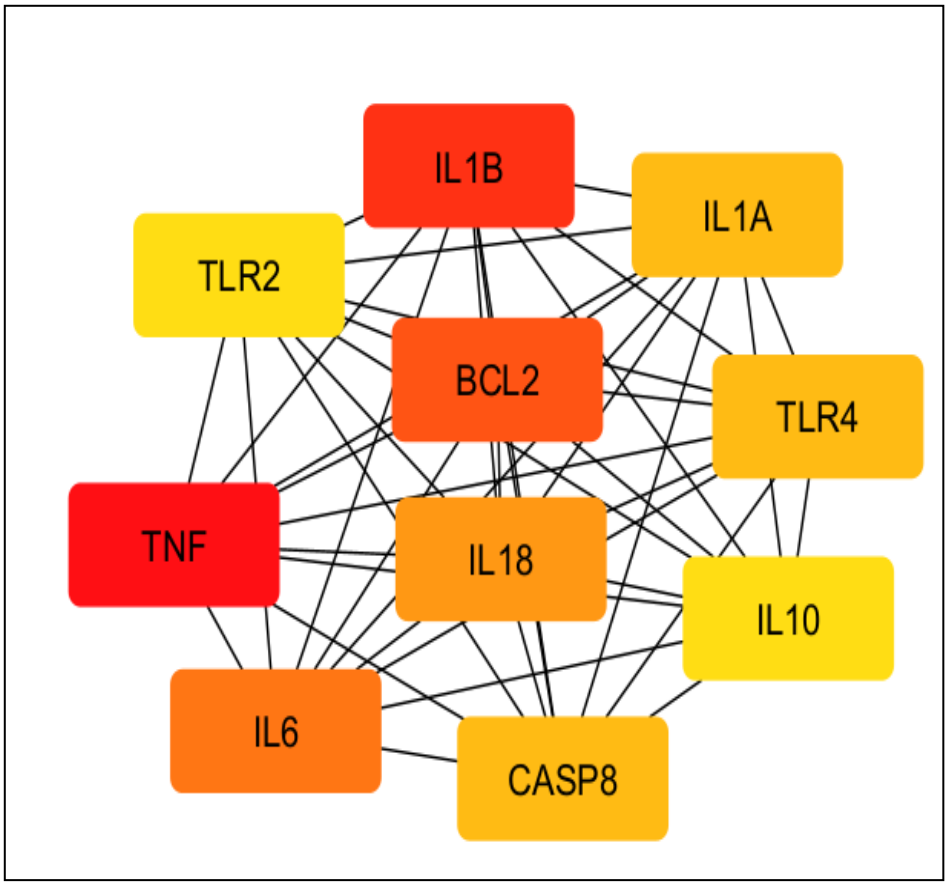

Figure 7.3.10: Identification of hub genes from PPI network using Cytoscape plugins Cytohubba.

Table 7.3.4: Top 10 selected HUB gene through degree method

Rank	Name	Score
1	TNF	47
2	IL1B	45
3	BCL2	44
4	IL6	43
5	IL18	42
6	IL1A	40
6	CASP8	40
6	TLR4	40
9	TLR2	39
10	IL10	39

Discussion

The insights gleaned from the findings presented in this chapter shed light on the gene expression patterns associated with the apoptotic pathway. Analysis of mRNA expression levels of key apoptotic and metastatic markers, such as *BAX, BCL2, MMP2/9, CASP3, CASP9, CASP8, IL10,* and *IL4,* provides valuable insights into the underlying mechanisms of action of *Solanum virginianum* (*Sv*) plant extract, melatonin, and their combination on breast cancer cells.

Across various treatment groups, there was a consistent pattern of upregulation of *BAX* and downregulation of *BCL2* and *MMP2/9*, indicating an induction of apoptosis and inhibition of metastasis. Additionally, there was an observed upregulation of *CASP3, CASP9,* and *CASP8,* further supporting the activation of apoptotic pathways. The modulation of *IL10* and *IL4* expression suggests a potential immunomodulatory effect of the treatments, with implications for the tumor microenvironment. Overall, these findings provide valuable insights into the molecular mechanisms underlying the effects of *Sv* plant extract, melatonin, and their combination on breast cancer cells, particularly in terms of apoptosis induction and metastasis inhibition.

In the case of MCF-7 cells, the notable upregulation of *BAX*, a pro-apoptotic protein, across all treatment groups suggests that *Solanum virginianum* plant extract, melatonin, and their combination induce apoptosis in breast cancer cells (Lopez et al., 2022). The increased expression of *BAX* is indicative of enhanced apoptotic signalling, ultimately leading to cell death (Yuan et al., 2022). Conversely, the downregulation of anti-apoptotic *BCL2* and metastatic markers *MMP2/9* in all treatment groups further supports the apoptotic and anti-metastatic effects of the treatments (Vihinen et al., 2018). The reduced expression of *BCL2* inhibits its anti-apoptotic function, thereby contributing to apoptosis induction, while the

diminished expression of *MMP2/9* suggests the inhibition of metastatic potential (Dofara et al., 2020; Jiang et al., 2021).

The upregulation of caspase-3 (*CASP3*) and caspase-9 (*CASP9*) mRNA expression in all treated groups indicates activation of apoptotic pathways (Boice and Bouchier-Hayes, 2020). *CASP3* serves as a key effector caspase involved in the execution phase of apoptosis, while *CASP9* acts as a critical initiator caspase in the intrinsic apoptotic pathway (Asadi et al., 2022; Yadav et al., 2021; Araya et al., 2021). The higher expression of *CASP3* and *CASP9* in combinational groups suggests synergistic effects, potentially amplifying apoptotic signalling (Huang et al., 2019).

Although *CASP8* mRNA expression was upregulated in all treated groups except the melatonin-treated groups, the combinational group exhibited higher expression than individual treatments. *CASP8* is involved in extrinsic apoptotic pathways, and its upregulation further supports the activation of apoptosis by the combination treatment (Mandal et al., 2020; Orning & Lien et al., 2021).

The modulation of interleukin-10 (*IL10*) and interleukin-4 (*IL4*) expression suggests an immunomodulatory effect of the treatments (Toney et al., 2022). Additionally, previous findings suggest that IL-4 induces apoptosis via *CASP3* activation (Quan et al., 2022). *IL10*, known for its anti-inflammatory properties, showed comparatively higher expression in all groups except for the combinational group with IC_{50} concentrations. This may indicate a shift towards an anti-inflammatory microenvironment in the treated cells (Najafi et al., 2019).

Conversely, *IL4* expression was elevated in all groups compared to the control. However, there were no significant differences among individual treatments and combinational groups, indicating that *IL4* expression may not be influenced by treatment type.

In the case of MDA-MB-231 cells (TNBC ells), *BAX* expression was upregulated across all treatment groups, with the highest level observed in the combinational IC_{50} group. Although the reduction in *BCL2* expression was not statistically significant, it further supports the pro-apoptotic shift in the treated TNBC cells (Adinew et al., 2023). This shift indicates that the treatments effectively target pathways involved in promoting cell survival and proliferation (Adinew et al., 2023).

Moreover, there was an observed increase in *CASP3, CASP8,* and *CASP9* mRNA expression, particularly in the combinational IC_{50} group, underscoring the activation of apoptotic pathways (Huang et al., 2019). The significant upregulation of *CASP8* and *CASP9* highlights the efficacy of the treatments in triggering intrinsic and extrinsic apoptotic pathways, potentially enhancing the overall apoptotic response in TNBC cells (Adinew et al., 2023).

*MMP*2 and *MMP9* contribute to breast cancer progression by facilitating the epithelial-to-mesenchymal transition, allowing mesenchymal cells to invade tissues and travel to distant locations by degrading the extracellular matrix and releasing growth factors and cytokines (Zhang et al.2019, Cheng et al.,2014, Lamouille & Derynck.,2014; Murray,2024; Xu et al.,2024). The downregulation of MMPs expression in all treatment groups suggests a potential inhibition of metastatic processes in TNBC cells (Chien et al., 2018). The increase in *IL4* expression in selected treatment groups and the varied response of *IL10* expression suggests a complex modulation of the immune microenvironment by the treatments. IL-4 is known to have both pro- and anti-tumorigenic effects, depending on the context, and its upregulation may indicate a potential immunomodulatory response elicited by certain treatments (Tzang et al., 2020; Liu et al., 2021). Conversely, the differential regulation of *IL10* expression underscores the complexity of cytokine-mediated signalling in the tumour

microenvironment and warrants further investigation into its specific role in TNBC (Chang et al., 2021; Chen et al., 2021).

Based on the findings of the gene expression studies, we conducted biochemical pathway analysis for target genes using PPI network construction using Cytohubba online software (Szklarczyk et al.,2023). A total of 57 genes and 778 interactions were identified. Based on the degrees of interactions,10 Hub genes were preferentially listed. It is important to note that *IL10, CASP8* and *BCL2* have been identified with a higher degree of interactions indicating their involvement in the anti-proliferative action of *Sv* leaf extract and/or melatonin. Studies have shown that *CASP8* is an important protein whose activation leads to upregulation of *CASP3* which is a critical point in the induction of apoptosis (Liu et al.,2023). Further, due to activation of apoptotic markers which leads downregulation of *BCL2* is also known to be involved in the activation of *APAF1* which signals *CASP9* to terminally activate *CASP3* cascade (Toney et al., 2022). Additionally, *IL10* activation along with other interleukins (Figure Chapter 7 gene expression graph of *IL4* and *IL10*) is known to modulate inflammatory circuit that is upregulated in breast cancer cells (Jain et al.,2023).

Overall, the findings highlight the multi-faceted effects of the treatments on breast cancer cells, including the induction of apoptosis, inhibition of metastatic potential, and modulation of the immune microenvironment. In summary, the mRNA expression data provide compelling evidence for the anti-cancer effects of Solanum virginianum plant extract, melatonin, and their combination, underscoring their potential as novel therapeutic agents for breast cancer.

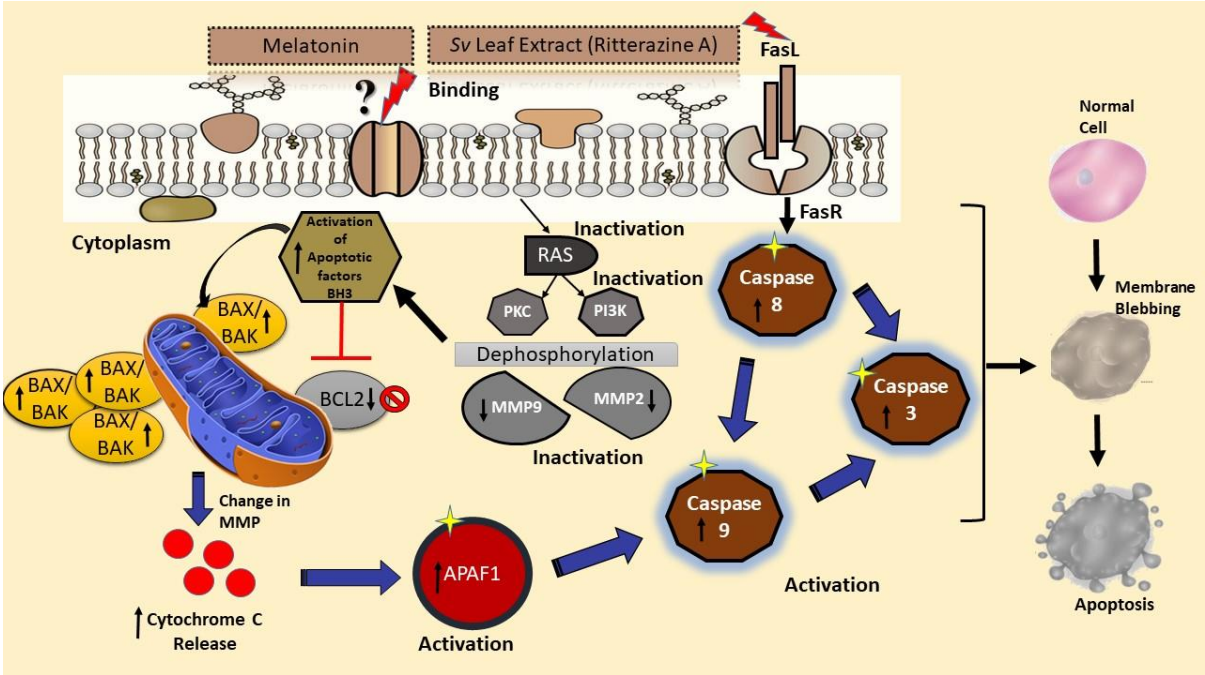

Comprehensive diagrammatic summary of molecular pathways possibly influenced by combinational treatment of *Sv* leaf extract and melatonin in Breast cancer